FACTA UNIVERSITATIS (NIŠ)
SER.: ELEC. ENERG. vol. 21, no. 2, August 2008, 195-207

# Sliding Mode Control Technique for an Induction Motor Drive Supplied by a Three-Level Voltage Source Inverter

**Sergey Ryvkin, Richard Schmidt-Obermöller, and Andreas Steimel**

**Abstract:** The possibility of using sliding-mode (SM) technique for an induction motor drive with a class of inverters dedicated to high power, the three-level voltage-source inverter (3LVSI), has been presented. A designed control based on the proposed two-step design procedure is discussed; drive simulation results are shown.

**Keywords:** Induction motor, sliding-mode control, switch mode, three-level voltage-source inverters.

## 1 Introduction

SLIDING-MODE control, Switch mode, Three-level voltage-source inverters [1–4]. It bases on using main characteristics of modern inverter semiconductor switches as Insulated Gate-Commutated Transistors (IGCTs) or Insulated-Gate Bipolar Transistors (IGBTs) that are operating in switch mode with distinctly higher switching frequency [5] than formerly used Gate-Turn-Off Thyristors (GTOs). The switch-mode operation of the devices contributes to high efficiency of the equipment, but has the adverse effect of complicating the control plant. In this case the IM drive with converter can be regarded as a nonlinear variable-structure system, and it is useful to exploit the principal operational mode of this class of control systems "sliding mode" for solving the control task. Sliding-mode control

Manuscript received on December 25, 2007.

S. Ryvkin, Prof., Ph.D., Dr.Sc., Senior Member IEEE, Leading Reseacher - Traneznikov Institute of Control Sciences of Russian Academy of Sciences, Laboratory of Adaptive Control Systems for Dynamic Objects, Profzoyuznaya, 65, 117997 Moscow, Russia (e-mail: rivkin@ipu.rssi.ru). R. Schmidt-Obermöller, Dipl.-Ing, Ruhr-University Bochum, Institute for Electrical Power Engineering and Power Electronics, D-44780 Bochum, Germany (e-mail: schmidt-o@eele.rub.de). Andreas STEIMEL, Prof. Dr.-Ing., VDE, Senior Member IEEE, Ruhr-University Bochum, Head of Institute for Electrical Power Engineering and Power Electronics, D-44780 Bochum, Germany (e-mail: steimel-o@eele.rub.de).

(SM) control technique allows to decompose the control design task and to design a control that shows low sensitivity to disturbances and plant parameter variations and gives a system high dynamics and accuracy. Many different control solutions for such drives based on SM control were proposed [1–4].

Today a standard item of modern high-power drives (rated power $> 3...4$ MW) is the IM fed by three-level inverters (3LVSI) [6]. The main feature of 3LVSI distinguishing from the classical voltage-source inverter with two possible voltage levels is an additional middle potential of the dc link. On the one hand it offers benefits as a superior harmonic spectrum for a given device switching frequency, low voltage stress at the cable and the end windings of motors, a low common-mode voltage, and substantially lower semiconductor switching losses. From the control point of view such a control scheme has a variable structure. Due to the complexity of this variable non-linear drive structure having a series coupling of the two nonlinear objects 3LVSI and IM different by nature, various control techniques were proposed, such as e.g. Field-Oriented Control [7], Direct Self Control and Indirect Stator-Quantity Control [8, 9] or Direct Torque Control [1, 10, 11]. But nearly all these techniques have in common the decomposition of the main high-order control task to several separated lower-order tasks, using linear control technique and heuristic solutions.

On the other hand, SM control could be successfully used for solving the control task in the frame of the principal operational mode of this class of variable-structure systems, due to its property of order reduction and its low sensitivity to disturbances and plant parameter variations [12]. The aim of this paper is to extend the SM technique to a the class of nonlinear control plants, dedicated especially to high-power drives: IM drives supplied by 3LVSIs.

The paper can be outlined as follows. The main part deals with the SM control design. First of all, such well-known descriptions as the two-phase equivalent model of a symmetrical balanced squirrel-cage IM in the stationary reference frame $(\alpha, \beta)$ and with rotor quantities referred to stator [13] and the canonical schema of the neutral-point-clamped 3LVSI with three-state semiconductor switches [6] are presented and discussed. Secondly, the backgrounds of SM used are briefly introduced. Third the control task is formulated and a two-step SM-control design technique suggested. The design results in the SM control for the above-mentioned drive system as the logical table for 3LVSI switch control and the conditions for the input voltage selection of the 3LVSI is given. At the end, results of a numerical simulation illustrating the properties of the suggested SM control are presented, followed by conclusions.

## 2 Control Plant Description

### 2.1 Used IM description

The classic model of a symmetrical balanced squirrel-cage induction machine in the stationary reference frame $(\alpha,\beta)$ and with the rotor quantities referred to stator [13] for SM control design is used:

$$\begin{aligned}
\frac{d\omega/p}{dt} &= \frac{1}{J}(M-M_L)\\
\frac{d\Psi_{s\alpha}}{dt} &= -R_s\cdot i_{s\alpha}+u_{s\alpha}\\
\frac{d\Psi_{s\beta}}{dt} &= -R_s\cdot i_{s\beta}+u_{s\beta}\\
\frac{i_{s\alpha}}{dt} &= \frac{1}{\sigma}\left(\frac{R_r}{L_sL_r}\Psi_{s\alpha}+\frac{p}{L_s}\omega\Psi_{s\beta}\right)-p\omega i_{s\beta}-\frac{\gamma}{L_s}i_{s_\alpha}+\frac{1}{L_s}u_{s\alpha}\\
\frac{i_{s\beta}}{dt} &= \frac{1}{\sigma}\left(\frac{R_r}{L_sL_r}\Psi_{s\beta}+\frac{p}{L_s}\omega\Psi_{s\alpha}\right)-p\omega i_{s\alpha}-\frac{\gamma}{L_s}i_{s_\beta}+\frac{1}{L_s}u_{s\beta}\ ,
\end{aligned} \tag{1}$$

where $\omega$ is the electrical angular velocity; $J$ the inertia and $M$ the electromagnetic torque

$$T = 3p\left(\Psi_{s\alpha}i_{s\beta}-\Psi_{s\beta}i_{s\alpha}\right)/2\ , \tag{2}$$

$M_L$ is the load torque; $\Psi_s^T = \left(\Psi_{s\alpha},\Psi_{s\beta}\right)$ the stator flux space vector; $i_s^T = \left(i_{s\alpha},i_{s\beta}\right)$ the stator current space vector; $u_s^T = \left(u_{s\alpha},u_{s\beta}\right)$ the stator voltage space vector; $R$ and $L$ denote resistance and self inductance, subscripts s and r stand for stator and rotor; $p$ is the pole number; $\sigma = 1-L_m^2/L_sL_r$, with $L_m$ being the mutual inductance is the leakage factor: $\gamma = L_sR_r/(L_r-R_s)$

### 2.2 Used 3LVSI description

The 3LVSI model depicted in Fig. 1 has three input rail: the positive (L+) and the negative (L-) ones of the dc link and the middle potential (M) between positive and negative potential (neutral point). The output terminals a, b, c can be connected to one from them by using three three-position switches (S1, S2, S3). The switch has three positions: (+) means the connection with the positive rail, (-) with the negative one and (0) with the neutral point.

There are 27 possible switching combinations. If the middle potential is balanced $(E_1 = E_2)$ there are 19 different output voltage space vectors with four different magnitudes, parts of them multiply redundant (Fig. 2). Next to the output vector position the switches combination is given.

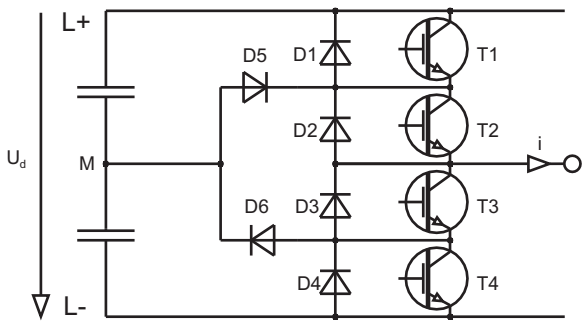


Fig. 1. Canonical schema of neutral-point-clamped 3LVSI

There are six full-voltage space vectors (A) with magnitude $B_A = 2U_d/3$, where $U_d = E_1 + E_2$; six intermediate-voltage space vectors (Z) with magnitude $B_Z = \sqrt{3}U_d/3$; six half-voltage space vectors with magnitude $B_H = U_d/3$, attained redundantly by two switch combinations, and the zero-voltage vector (N), with three possible switch combinations.

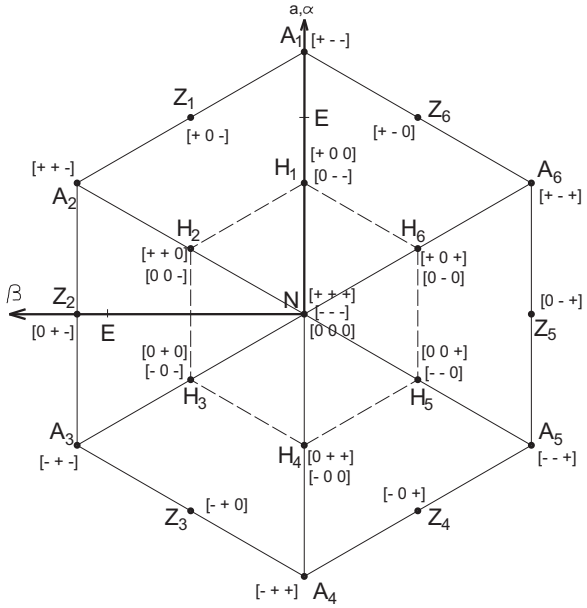


Fig. 2. Voltage space-vector diagram of 3LVSI

Only these above mentioned 19 different output-voltage space vectors can be used in the discontinuous control.

## 3 SM backgrounds

SM is a special motion of the closed-loop relay system, when the relay switches between its two positions with a switching frequency, distinctly higher than the motor short-circuit time-constant [3]. By a correctly selected switching function $F$ the system has good dynamic, low sensitivity to disturbances and plant parameter variations. Usually the switching function $F$ has been selected as an error function of the control variables and it must be led to zero $(F \rightarrow 0)$. Formally, the system state must reach a sliding surface or manifold

$$F = 0 \tag{3}$$

and slides then on the manifold into the zero point, independently of the system dynamic. A typical SM control has the form

$$u = -U(x)\,\mathrm{sgn}(F)\ ,\ u \in R^m\ , \tag{4}$$

where $x$ is the system state vector, $x \in R^n, n \geq m$ , $U(x)$ is the square diagonal matrix of the control magnitudes, $E \in R^m$. The system state reaches the sliding manifold (3) in finite time from the initial condition, which has been bounded by the value of the constituent of matrix $U(x)$, and keeps to it. This magnitude bounds the uncertainty of the system, the load value unto which the system is commonly robust. and then slides on the manifold into the zero point independently of the system dynamic.

## 4 SM Control Design

### 4.1 Two-step control design

The main control aim of the IM drive will be satisfied, if the average value of the mechanical output variable (for example rotor speed or position) will equal the set value, which has subscript z. But this task in an obvious or implicit kind is reduced to the task of maintaining the target torque M at the shaft of the motor. As the number of the independent controls is equal to the order of the control space, in our case the voltage plane, and higher as one, it is first of all possible to control two variables: not only one mechanical variable, but another variable which describes electrical or power requirements of the IM. Usually the stator-flux modulus $|\Psi_s| = \sqrt{\Psi_{s\alpha}^2 + \Psi_{s\beta}^2}$ is chosen. In this case the error function $F$ is formed as

$$F = \begin{vmatrix} F_\Psi \\ F_M \end{vmatrix} = \begin{vmatrix} |\Psi_{sz}| - |\Psi_s| \\ M_z - M \end{vmatrix} \tag{5}$$

and the control aim is

$$F = 0\,. \tag{6}$$

While the IM drive is a variable-structure system with discontinuous control, one of the possible ways for reaching Eq.(6) is organizing a sliding motion on the manifold (5), (6), i.e. the solving the control task, by using the output-voltage space vectors of the 3LVSI. In this case the error function $F$ (5) plays the role of the switching function of the structures. It is a function of the system variables and guarantees, that the system state "slides" on the manifold into the zero point, independently of the system dynamic.

The special feature of the IM drive as a non-linear system with discontinuous control is that the number of the discontinuous controls is bigger than the control order, and that they are constant and cannot be changed. The main problem of the control design is the synthesis of the switching law that guarantees sliding on the manifold (5), (6), i.e. the solving the control task, by using the output-voltage space vectors of the 3LVSI.

In this case the two-step control design technique [2] is fruitful. It allows to solve the design task for the 3LVSI that has 19 different output-voltage space vectors by a two-dimensional control space. The main idea of this technique is to take the nonlinearities of IM and 3LVSI separately into account. At the first step only the IM model is used with a two-dimensional control

At the second step the real discontinuous output voltage of 3LVSI is taken into account, and the realization task of the SM is solved with. As results there are the logical table for the switch control and the conditions for the 3LVSI input-voltage selection.

### 4.2 Fist design step

The control task is solved by using the equation of the error-function variation and the IM model (1)

$$\begin{aligned}\frac{d}{dt}\begin{vmatrix}F_\Psi\\F_M\end{vmatrix} = &\begin{vmatrix}\frac{d|\Psi_{sz}|}{dt} + \frac{R_s\left(\Psi_{s\alpha}i_{s\alpha}+\Psi_{s\beta}i_{s\beta}\right)}{|\Psi_s|}\\ \frac{d|M_z|}{dt} + \frac{1}{\sigma}\left(\frac{\gamma}{L_s} + \frac{p}{L_s}\omega\Psi_s^2\right) - p\omega\left(\Psi_{s\alpha}i_{s\alpha} + \Psi_{s\beta}i_{s\beta}\right)\end{vmatrix} -\\ &-\begin{vmatrix}1 & 0\\ \frac{M}{|\Psi_s|} & \frac{1}{\sigma}\frac{|\Psi_s|}{L_s} + \frac{\left(\Psi_{s\alpha}i_{s\alpha}+\Psi_{s\beta}i_{s\beta}\right)}{|\Psi_s|}\end{vmatrix} \times \begin{vmatrix}u_\Psi\\u_M\end{vmatrix}\,,\end{aligned} \tag{7}$$

where $U_F^T = (u_\Psi, u_M)$ is the control vector, which is connected with the phase voltages by the transformation

$$\begin{vmatrix} u_a \\ u_b \\ u_c \end{vmatrix} = \begin{vmatrix} \cos\rho & -\sin\rho \\ \cos(\rho - \frac{2\pi}{3}) & -\sin(\rho - \frac{2\pi}{3}) \\ \cos(\rho + \frac{2\pi}{3}) & -\sin(\rho + \frac{2\pi}{3}) \end{vmatrix} \times \begin{vmatrix} u_\Psi \\ u_M \end{vmatrix} , \tag{8}$$

where $\rho = \arctan(\Psi_{s\alpha}/\Psi_{s\beta})$ is the stator-flux angle.

The sliding motion on the manifold (5), (6) can be designed by the control hierarchy method [3], because the error function $F_\Psi$ depends solely on control $u_\Psi$. The problem of sliding domain is thus reduced to a sequential analysis of two scalar cases. The scalar sliding-mode condition is

$$\lim_{F\to+0} \frac{dF}{dt} < 0 \ \ \& \ \ \lim_{F\to-0} \frac{dF}{dt} . \tag{9}$$

The above mentioned condition (9) will be fulfilled, if the control vector components $u_\Psi$ and $u_M$ are selected depending upon the sign of the components of the error function $F$:

$$u_\Psi = U_\Psi \mathrm{sgn}\,(F_\Psi) , \tag{10}$$

$$u_M = U_M \mathrm{sgn}\,(F_M) \tag{11}$$

and their magnitudes $U_\Psi$ and $U_M$ are selected as

$$U_\Psi \geq U_{\Psi eq} = \left| \frac{d|\Psi_{sz}|}{dt} + \frac{R_s\left(\Psi_{s\alpha} i_{s\alpha} + \Psi_{s\beta} i_{s\beta}\right)}{|\Psi_s|} \right| , \tag{12}$$

$$U_M \geq U_{Meq} = \left| \begin{array}{l} \frac{dM_z}{dt} - \frac{M}{|\Psi_{sz}|} \cdot \frac{d|\Psi_{sz}|}{dt} + \frac{1}{\sigma}\left(\frac{\gamma}{L_s} + \frac{p}{L_s}\omega\Psi_s^2\right) - \\ -\left(p\omega + \frac{R_s M}{\Psi_{sz}^2}\right)\left(\Psi_{s\alpha} i_{s\alpha} + \Psi_{s\beta} i_{s\beta}\right) \end{array} \right| \tag{13}$$

They bound the initial condition, from which the state will reach the sliding manifold in finite time, the uncertainty of the system and the load value to which the system is robust in general.

### 4.3 Second design step

The transfer from the control quantity $U_F$ to the real output voltages of a 3LVSI is based on the fact, that the choice conditions of the magnitudes of the formally entered controls in the stator-flux rotating-frame obey the inequalities (12), (13). It is obvious, if designing the real discontinuous voltage control thus that the voltages

projections on the axes of the stator-flux rotating frame have their marks and sizes, which are needed by the control algorithm with the formally entered controls, the sliding mode on crossing before the chosen surfaces will take place. Of course, the sizes of the projections will change during operation.

Control (10), (11) and inequalities (12), (13) determine in the control space rotating synchron'ously with the stator-flux four control areas $U_1^*, U_2^*, U_3^*, U_4^*$ with guaranteed sliding motion (Tab. 1): $U^* = \{U^*\} = U_1^* \cup U_2^* \cup U_3^* \cup U_4^*$ , $U_1^* \cap U_2^* = 0$ , $U_1^* \cap U_3^* = 0$ , $U_1^* \cap U_4^* = 0$ , $U_2^* \cap U_3^* = 0$ , $U_2^* \cap U_4^* = 0$ , $U_3^* \cap U_4^* = 0$

Table 1. Sliding mode control areas

| | $U_1^*$ | $U_2^*$ | $U_3^*$ | $U_4^*$ |
|---|---|---|---|---|
| sgn $F_\Psi$ | 1 | 1 | -1 | -1 |
| sgn $F_M$ | 1 | -1 | 1 | -1 |

By transformation (7) to the three-phase stator-winding-fixed frame (a, b, c) these four control areas do not change their form, but rotate with stator-flux angular velocity $\omega = \frac{d\rho}{dt}$ (see Fig. 3)

SM will be secured by using the discontinuous voltages of the 3LVSI, if each control area includes at any time at minimum one of the 3LVSI output-voltage vectors. Calculating the 3LVSI dc-link voltage and transferring the control (10), (11) to the switching control of 3LVSI switches is based on this condition. Both

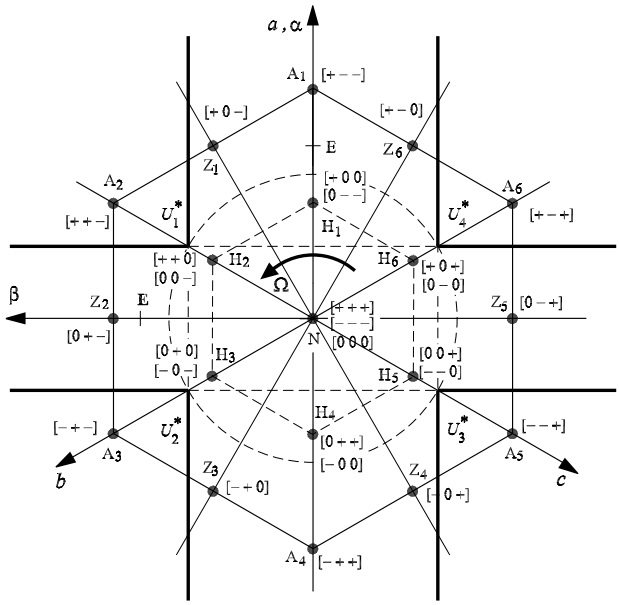


Fig. 3. SM control areas and voltage space vectors of 3LVSI

are performed by the following assumptions:

- The selected control magnitudes $U_\Psi$ and $U_M$ are equal: $U_\Psi = U_M = U$.
- The used 3LVSI output-voltage space vectors are only full ones and intermediate ones (in this first step of investigation).
- The value of the 3LVSI dc-link voltage must be the minimal possible.
- The value of the 3LVSI dc-link voltage has been calculated, using the magnitude of the intermediate voltage space vectors. In this case the dc-link voltage value is $B_A - B_z = \left(2-\sqrt{3}\right) U_d/3$

By these assumptions the selection condition of the 3LVSI input dc-voltage value is according to geometrical reasons:

$$\arcsin\left(U/B_z\right) \leq \pi/6 \;, \tag{14}$$

and the 3LVSI dc-link voltage value can be calculated as

$$U_d \geq 2\sqrt{3}\cdot U \;. \tag{15}$$

The control strategy guaranteeing that each time in each of the four control areas $U_1^*, U_2^*, U_3^*, U_4^*$ will be at least one of the twelve 3LVSI output-voltage space vectors is presented in the Tables 2 and 3. It connects the signs of the control errors sgn $F_M$ and sgn $F_\Psi$ and the control $S_a$, $S_b$, $S_c$ of the phase three-positions switches S1, S2 and S3, in dependence upon the stator-flux position in one of the twelve $\pi/6$ - sectors.

Table 2. Switch controls I

| $\rho$ | $S_a$ | $S_b$ | $S_c$ |
|---|---|---|---|
| $(0\ldots\pi/6)$ | sgn $F_\Psi$ | sgn $F_M$ | C |
| $(\pi/6\ldots\pi/3)$ | D | sgn $F_M$ | $-$sgn $F_\Psi$ |
| $(\pi/3\ldots\pi/2)$ | $-$sgn $F_M$ | A | $-$sgn $F_\Psi$ |
| $(\pi/2\ldots2\pi/3)$ | $-$sgn $F_M$ | sgn $F_\Psi$ | B |
| $(2\pi/3\ldots5\pi/6)$ | C | sgn $F_\Psi$ | sgn $F_M$ |
| $(5\pi/6\ldots\pi)$ | $-$sgn $F_\Psi$ | D | sgn $F_M$ |
| $(\pi\ldots7\pi/6)$ | $-$sgn $F_\Psi$ | $-$sgn $F_M$ | A |
| $(7\pi/6\ldots4\pi/3)$ | B | $-$sgn $F_M$ | sgn $F_\Psi$ |
| $(4\pi/3\ldots3\pi/2)$ | sgn $F_M$ | C | sgn $F_\Psi$ |
| $(3\pi/2\ldots5\pi/3)$ | sgn $F_M$ | $-$sgn $F_\Psi$ | D |
| $(5\pi/3\ldots11\pi/6)$ | A | $-$sgn $F_\Psi$ | $-$sgn $F_M$ |
| $(11\pi/6\ldots2\pi)$ | sgn $F_\Psi$ | B | $-$sgn $F_M$ |

Such a control (3LVSI dc-link voltage value and control table) guarantees that the system will reach - from the initial condition selected in (12), (13) - the sliding

Table 3. Switch controls II

| sgn $F_\Psi$ | 1 | 1 | -1 | -1 |
|---|---|---|---|---|
| sgn $F_M$ | 1 | -1 | 1 | -1 |
| A | 1 | 0 | 0 | -1 |
| B | 0 | -1 | 1 | 0 |
| C | -1 | 0 | 0 | 1 |
| D | 0 | 1 | -1 | 0 |

manifold (5), (6) in finite time and remains on it and will be robust against the load value variation, the selected uncertainty of the system parameters, of the 3LVSI dc-link voltage and of the estimation of the stator-flux angle position.

## 5 Results of the numerical simulation

This SM control was tested in a simulation of the IM drive fed by a 3LVSI [14], the characteristics of which are presented in Tab. 4.

Table 4. Characteristics of IM drive for Simulation

| Parameter | Symbol | Value |
|---|---|---|
| Rated power (kW) | $P_N$ | 180 |
| Rated voltage (V) | $U_N$ | 600 |
| Rated current (A) | $I_N$ | 180 |
| Rated speed (rad/s) | $\omega_N$ | 150 |
| Rated torque (Nm) | $M_N$ | 580 |
| Rated flux linkage (Wb) | $\lvert\Psi_{sz}\rvert$ | 1.71 |
| Stator resistance ($m\Omega$) | $R_s$ | 25.9 |
| Rotor resistance ($m\Omega$) | $R_r$ | 18 |
| Mutual inductance (mH) | $L_\mu$ | 27.6 |
| Leakage inductance (mH) | $L_\sigma$ | 1.3 |
| Numper of pole pairs | $p$ | 2 |
| DC-link rated voltage (V) | $U_d$ | 422 |
| Maximal switch frequency (Hz) | $f_{c\max}$ | 500 |
| Control cycle time ($\mu s$) | $T_c$ | 200 |

The 3LVSI state is determined by the sliding-mode controller that uses as input signals the error signs (10), (11) and the information about the stator-flux position and produces the output signals, using Tables 2 and 3. In a first step, the design of the sliding-mode controller uses only the full and intermediate voltage space-vectors, which are needed in the upper speed range. The flux and torque hysteresis bands were set to 7% and 3.5% of the rated value respectively. Speed was held constant at 104 rad/s, torque was set up to 30% of the rated break-down value, which is equal to the rated value. At $t = 0\ s$, flux is commanded to its rated value, and at $t = 0.03\ s$, torque is commanded to the rated value. The simulation was carried out

in real physical variables, but they are presented in per unit (p.u.) system. Only the time (the figures horizontal scale) is SI unit (s).

Fig. 4 shows the alpha/beta components of the stator-flux space vector and the torque.

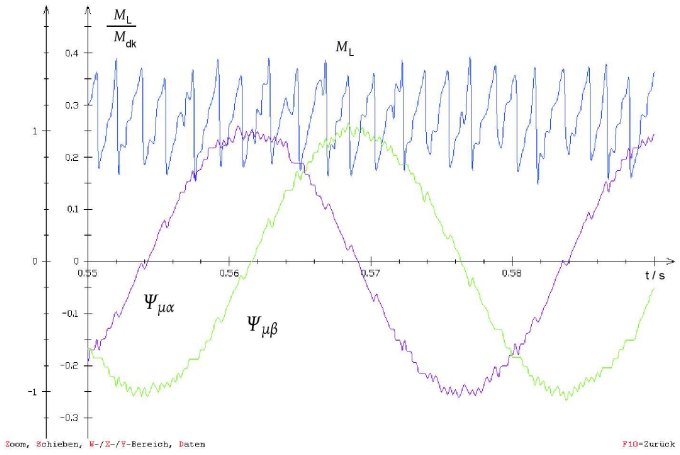


Fig. 4. Torque and alpha/beta component of stator-flux space vector

In Fig. 5 the discrete output-voltage space vectors and the circular trajectory of the stator-flux space-vector are pictured.

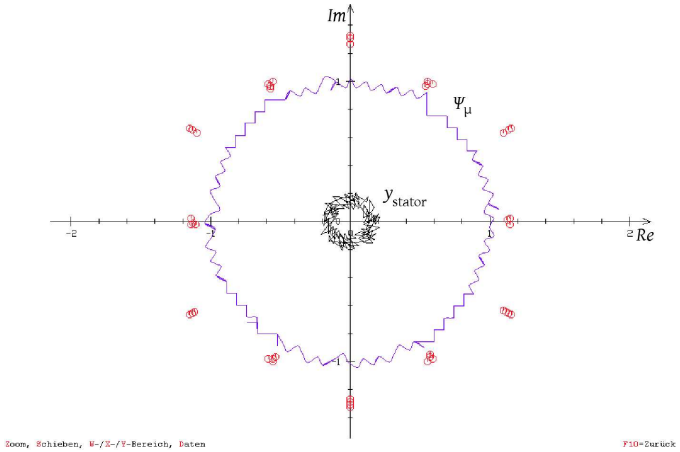


Fig. 5. Root locus of stator-flux, stator-current and stator-voltage space vectors

Fig. 4 shows that the torque at the speed 104 $rad/s$ is a slightly erratic

## 6 Conclusion

SM technique has been extended to IM drives supplied by 3LVSIs. A new approach to the control design of IM drives with 3LVSIs with high-voltage power semiconductor switches is presented. The designed SM control gives the drive all advantageous characteristics of SM control as high dynamic, low sensitivity to disturbance of both the load and the input dc-link voltage and to plant parameter variations. The simulation confirms highly dynamic behavior, accuracy, simplification of the control algorithm and reduction of the computing capacity requirements of the controller.

The next steps in the implementation of the SM control design are removing some of the assumed restrictions, i.e. equal magnitudes $U_\Psi$ and $U_M$ and others, and using the half-voltage and zero-voltage space vectors by complete design of the controller. Such a solution will improve the control quality, but needs the development of the new design technique and receiving additional information about the position of the equivalent control.

### Acknowledgments

The kind sponsorship of the research visit of Prof. Sergey Ryvkin at the Institute for Electrical Power Engineering and Power Electronics of Ruhr-University Bochum by the German Academic Exchange Service, Bonn, is gratefully acknowledged.

## References

[1] C. Lascu, I. Boldea, and F. Blaabjerg, "Variable-structure direct torque control, a class of fast and robust controllers for induction machine drive," *IEEE Trans. Ind. Electron.*, vol. 51, no. 4, pp. 785–792, 2004.

[2] S. Ryvkin, "Sliding mode technique for ac drive," in *Proc.10th Int. Power Electron. & Motion Control Conf., EPE - PEMC*, Dubrovnik & Cavtat, Croatia, 2005.

[3] V. I. Utkin, J. Gldner, and J. Shi, *Sliding mode control in electromechanical system*. London, Philadelphia: Taylor & Francis, 1999.

[4] J. Vittek, M. Stulrajter, P. Makys, I. Skalka, and M. Mienkina, "Microprocessor implementation of forced dynamics control of permanent magnet synchronous motor drives," in *Proc. 10th Int. Conf. Optimization of Electrical and Electronic Equipment, OPTIM 2006*, vol. III, Brasov, Romania, 2006, pp. 3–8.

[5] B. K. Bose, *Power electronics and motor drives - advances and trends*. Burlington: Academic, 2006.

[6] A. Nabae, I. Takahashi, and H. Akagi, "A new neutral-point-clamped PWM inverter," *IEEE Trans. Ind. Applicat.*, vol. 17, no. 5, pp. 518–523, 1981.

[7] F. Blaschke, "The principle of field orientation as applied to the new transvector closed-loop control system for rotating-field machines," *Siemens Rev.*, vol. 39, pp. 217–220, 1972.

[8] M. Depenbrock, "Direct self-control (DSC) of inverter-fed induction machine," *IEEE Trans. Power Electron.*, vol. 3, no. 4, pp. 420–429, 1988.

[9] A. Steimel, "Stator-flux-oriented high performance control in traction," in *35th Annual Meeting IEEE IAS Industry Application Society*, vol. Tutorial H-4, Rom, 2000.

[10] G. S. Buja and M. P. Kazmierkowski, "Direct torque control of PWM inverter-fed AC motor - a survey," *IEEE Trans. Ind. Electron.*, vol. 51, no. 4, pp. 744–757, 2004.

[11] P. Tiitinen, P. Pohjalainen, and J. Lalu, "The next generation motor control method: Direct torque control (DTC)," *EPE Journal*, vol. 5, no. 1, pp. 14–18, 1995.

[12] S. Ryvkin, R. Schmidt-Obermöller, and A. Steimel, "Formal derivation of sliding mode control for high power induction-motor drives fed by three-level voltage source inverters," in *Proc. 16th Int. Conf. Electrical Drive and Power Electron., EDPE 2007*, The High Tatras, Slovakia, 2007.

[13] W. Leonhard, *Control of electrical drive*, 3rd ed. Berlin: Springer-Verlag, 2001.

[14] E. Krafft, A. Steimel, and J. K. Steinke, "Three-level high-power inverters with IGCT and IGBT elements compared on the basis of measurements of the device loses," in *Proc. 8th European Conference on Power Electronics*, Lausanne, Schwitzerland, 1999.